Applied Catalysis, 9 (1984) 225—233
Elsevier Science Publishers B.V., Amsterdam — Printed in The Netherlands

CHARACTERIZATION OF SUPPORTED VANADIUM OXIDE CATALYSTS BY LOW TEMPERATURE OXYGEN CHEMISORPTION TECHNIQUE: I. THE V_2O_5/γ-Al_2O_3 SYSTEM

N.K. NAG[a], K.V.R. CHARY, B. Mahipal REDDY, B. Rama RAO and V.S. SUBRAHMANYAM[b]
Catalysis Section, Regional Research Laboratory, Hyderabad 500 009, India.

[a]Present address: Department of Fuels Engineering, University of Utah, Salt Lake City, Utah 84112, USA.
[b]Enquiries regarding this paper should be addressed either to V.S.S. or to N.K.N.

(Received 9 May 1983, accepted 8 November 1983)

ABSTRACT

Low temperature oxygen chemisorption (LTOC) has been applied to characterize γ-Al_2O_3 supported vanadium oxide catalysts. The results strongly suggest the formation of a monolayer with high dispersion of V-oxide on the alumina surface. The monolayer coverage of the surface is completed when the V_2O_5 content of the catalysts reach 11.9% and beyond this loading crystallites of V_2O_5 start to form on the alumina surface. Within the monolayer level the active surface area and active site density are found to increase with increased vanadia loading, while those in the 'post monolayer' region show a sharp decline as the load increases. The dispersion of vanadia remains essentially constant within the monolayer level and decreases almost linearly as a function of V_2O_5 loading in the post monolayer region. Information gathered from other techniques, including ESR, IR and surface area measurements, substantiate the results of LTOC experiments. Thus, LTOC technique is found to be a valuable tool for characterizing supported oxidation catalysts which are identified with redox properties.

INTRODUCTION

Vanadium oxides form a group of industrially important catalysts for the ammoxidation and partial oxidation of aromatic hydrocarbons [1,2] and much research activity has been devoted towards understanding the nature of active sites as well as the role played by the carrier of the supported catalysts. The most efficient utilization of any supported catalyst depends on the percent exposed or the dispersion of the active component on the surface of the support. This dispersion is often controlled, among other factors, by the extent of loading and the nature of the support. The actual state of the active component on the surface depends mainly on the method of preparation, the acidity of the support and the amount of the active component supported. The active component may remain as a highly dispersed monolayer or as crystallites on the support surface, or may even form a solid solution with the latter [2].

Extensive studies have been devoted to the understanding of the mechanism of formation and properties of V-oxide monolayer catalysts [2,3], as well as the role

0166-9834/84/$03.00

of V=O bonds [4,5] in the catalytic activities of vanadium oxide catalysts. Apparently, no effort has so far been made to estimate the active surface areas of the supported V-oxide catalysts. Weller et al. [6] were the first to demonstrate the applicability of LTOC in finding the active surface areas of supported Mo-oxide catalysts. Other works followed to prove the merits and demerits of this technique [7-12]. In this article we report similar studies with V-oxide systems. The purpose of this work has been twofold, first, to gain an idea about the state of V-oxide on the surface of the support and, second, to have an estimate on the active surface area and the site density on the surface.

EXPERIMENTAL

Pure crystalline V_2O_5 was prepared by decomposing ammonium metavanadate (E. Merck, Analar) at 450°C for 4 h in air. The supported catalysts were prepared by impregnating γ-Al_2O_3 (ACC, India) with stoichiometric aqueous solutions of ammonium metavanadate and evaporating to near dryness with constant stirring. The resulting paste was oven dried at 110°C for 16 h and calcined in air at 500°C for 4 h. The V content of the finished catalysts were determined by atomic absorption spectroscopy and are reported as wt% of V_2O_5 on Al_2O_3.

A conventional high vacuum glass system was used to measure the BET surface areas by N_2 (0.162 nm^2) adsorption at 77 K. The same system was employed to determine the pore size distribution by the BJH method [13]. X-ray diffractograms were recorded on a Philips PW 1051 diffractometer by using Ni-filtered CuK_α radiation. The most intense line of V_2O_5, corresponding to the (001) plane was taken for the line broadening measurements. Quartz (100) line was used for correction of the broadening by the instrument. The average crystal diameter was determined by the application of the Scherrer equation. All ESR experiments were performed under vacuum and at 109 K with a JEOL FE 3X, X-band (ν = 9.278 GHz) spectrometer with 100 KHz modulation. Self supporting KBr pellets containing the catalyst samples were used to scan the IR spectra on a Perkin Elmer 283B spectrometer at ambient conditions.

A modified version of the above mentioned high vacuum system (up to 10^{-6} Torr) with the option of reducing the samples by flowing hydrogen was applied for the LTOC experiments. The standard procedure employed was the reduction for 6 h followed by evacuation for 1 h (10^{-6} Torr), both at 500°C, prior to oxygen chemisorption. Before the introduction of oxygen, the system was further evacuated for 1 h at the temperature of oxygen chemisorption, 196 K. Purified oxygen from a storage bulb was then allowed to enter into the catalyst chamber with predetermined dead space and the first adsorption isotherm representing the sum of physisorbed and chemisorbed oxygen was determined in the usual way [6]. After this, the physisorbed oxygen was removed by evacuating (10^{-6} Torr) for 1 h at 196 K. Immediately after this a second isotherm representing only the physisorbed oxygen was generated

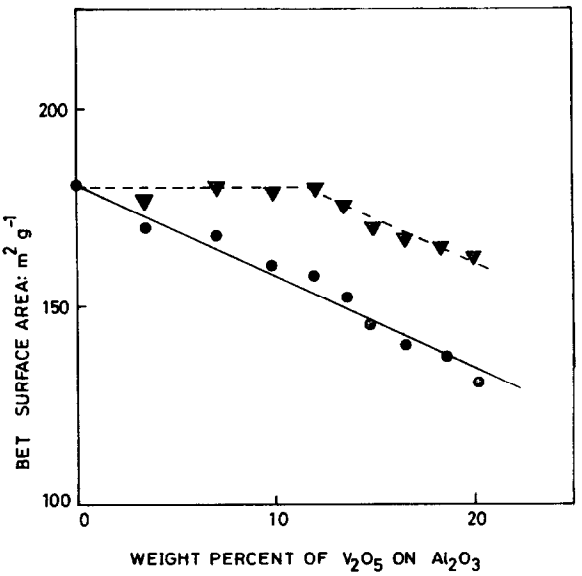

FIGURE 1 BET surface areas of the catalysts: ●——●; surface area based on unit weight of catalyst; ---▽---▽---, surface area based on unit weight of support.

in an identical manner. From these two isotherms, which were parallel at the pressure range used (120-250 Torr), the volume of chemisorbed oxygen was determined from the difference of their intercepts on the Y-axis [6]. The BET surface area of this reduced catalyst was determined and saved after evacuation for the ESR experiments.

RESULTS

Surface area and pore size distribution

The BET surface areas of the unreduced and the reduced catalysts are given in Figure 1 and Table 1 respectively. From Figure 1 it is observed that the surface areas of the unreduced catalysts based on unit weight of alumina remain constant up to a V_2O_5 loading of 11.9%, after which it decreases steadily. In contrast to this, the surface area based on unit weight of catalyst decreases with increasing vanadia content from the very beginning. The same trend is also observed for the reduced catalysts (Table 1). The average pore radius of the unreduced catalysts remained virtually constant at 4.3 ± 0.3 nm as compared with 3.4 nm for the support. Similarly the average pore volume of the catalysts were found to be 0.36 ± 0.02 ml g^{-1} as compared with 0.41 ml g^{-1} for the support. The small increase in the value of average pore radius and the corresponding decrease in the pore volume is probably due to the blocking of some micropores by V_2O_5.

TABLE 1

Unreduced catalyst		Reduced catalyst			
Catalyst composition: Wt% of V_2O_5 on Al_2O_3	V_2O_5 crystallite size nm	Active site density[a] nm^{-2}	Surface coverage[b]	BET surface area[c] $m^2\ g^{-1}$	Volume of oxygen chemisorbed, ml (STP) g^{-1} cat.
0.0	-	-	0.0	180.0	-
3.4	-	0.23	5.7	183.0	0.79
7.0	-	0.53	13.1	173.2	1.72
9.8	-	0.68	16.7	172.6	2.18
11.9	35.5	0.90	22.0	168.3	2.80
13.7	49.5	0.87	21.3	165.1	2.66
14.8	74.0	0.84	20.7	159.4	2.50
16.4	> 100.0	0.79	19.6	155.7	2.31
18.5	> 100.0	0.61	15.0	166.8	1.90
20.1	> 100.0	0.37	9.1	159.0	1.10
100.0	-	-	-	11.5	0.87

[a]This is equal to the number of oxygen atoms chemisorbed per unit area of the reduced catalyst.
[b]Defined as: 100 x (active surface area/BET surface area of the reduced catalyst.
[c]Based on unit weight of catalyst.

X-ray, IR and ESR

No characteristic XRD peak of V_2O_5 was detectable up to a loading of 11.9%; while the samples with higher vanadia content showed the XRD patterns which grew in intensity as the amount of V_2O_5 increased. The absence of the peaks at the lower concentration region can be taken as the indication of high dispersion of V-oxide on the support surface. Otherwise, if the crystallites are formed, they are less than 4 nm and are beyond the detection capability of the technique. The size of the crystallites increases rapidly above 100 nm when the load exceeds 16.4% (Table 1).

IR spectra of the catalysts with V_2O_5 content higher than 11.9% showed two characteristic bands of V_2O_5 at 1020 cm^{-1} and 825 cm^{-1} corresponding to V=O bond stretching and V-O-V deformation respectively. These bands, however, were not detected at lower loadings of V_2O_5. These results are in good agreement with other published results [4,5].

The ESR spectra of the reduced catalysts were recorded with an eye to gaining

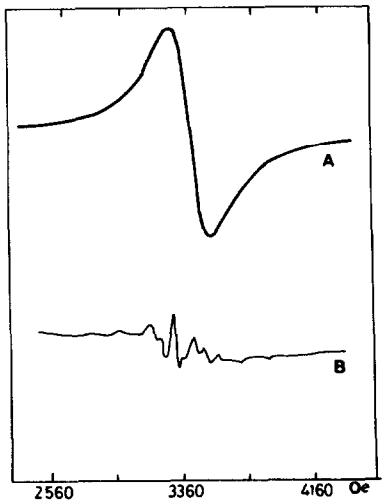

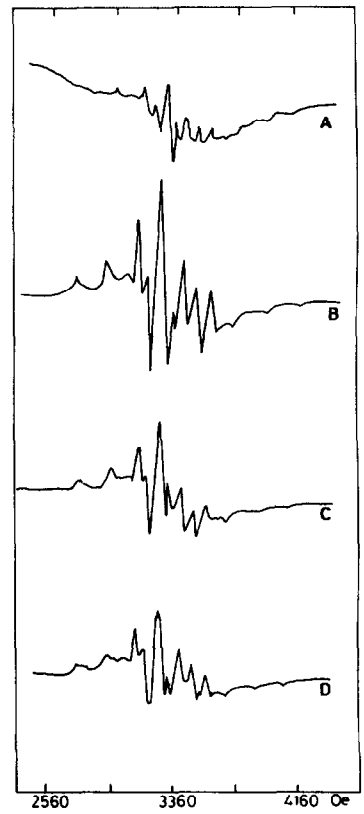

FIGURE 2 ESR spectra, recorded at 109 K and 10^{-6} Torr, of (A) pure V_2O_5; (B) 11.9% V_2O_5 on γ-Al_2O_3 (unreduced).

FIGURE 3 ESR spectra, recorded at 109 K and 10^{-6} Torr, of the reduced catalysts; (A) pure V_2O_5, (B) 3.4% V_2O_5, (C) 11.9% V_2O_5, and (D) 20.1% V_2O_5, all on γ-Al_2O_3.

some information on the valence state of vanadium on which chemisorption of oxygen occurs at 196 K. The spectra of pure V_2O_5 and 11.9% of V_2O_5/γ-Al_2O_3, both unreduced, are given in Figure 2, and those of the reduced catalysts are given in Figure 3. The important point to be noted is that while unsupported V_2O_5 shows a singlet ($g = 1.97$) at 109 K the supported vanadium oxide shows hyperfine splitting (hfs) due to V^{51} ($I = 7/2$). This hfs is of similar profile as that of the reduced catalysts (Figure 3). These results are in good agreement with other work [14,15]. The axially symmetrical g values and the hfs constants of the reduced catalysts remained practically constant and are given as follows: $g_{\perp} = 1.99$, $g_{11} = 1.94$, $A_{\perp} = 71$ G and $A_{11} = 192$ G.

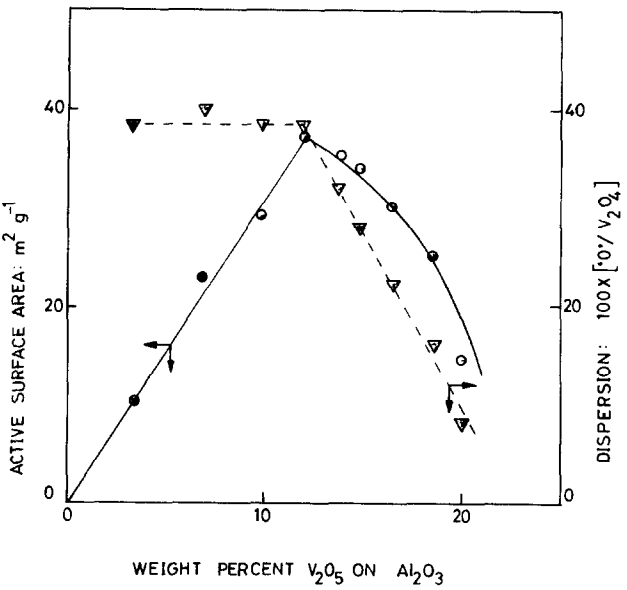

FIGURE 4 Active surface areas and dispersion of the supported catalysts as a function of V_2O_5 loading.

Low temperature oxygen chemisorption

Since oxygen failed to chemisorb on the oxidised form of the catalysts at 196 K it was necessary to reduce the catalysts to generate the surface on which the chemisorption could occur. Pure and unsupported V_2O_5 was reduced at different temperatures prior to oxygen chemisorption. No LTOC was observed up to 300°C of reduction. The amount of chemisorbed oxygen increased linearly as a function of reduction temperature in the range 300 to 500°C and then levelled off. Therefore, 500°C was chosen as the standard temperature of reduction by hydrogen. The volume (STP) of oxygen chemisorbed per g of various catalysts are given in Table 1. The factor for the conversion of unit volume of chemisorbed oxygen to the corresponding active surface area was determined by the method applied by Parekh and Weller [6] and is summarised as follows. Pure V_2O_5 was reduced at 500°C and oxygen was chemisorbed on it at 196 K. From the BET surface area of this reduced catalyst and the volume of oxygen chemisorbed the factor was determined from the following equation:

$$\text{factor} = \frac{\text{BET surface area } (m^2\ g^{-1}) \text{ of the reduced } V_2O_5 \text{ sample}}{\text{volume of oxygen (ml STP) chemisorbed } g^{-1}}$$

The factor was found to be 13.2 $m^2\ ml^{-1}$ of oxygen (STP) chemisorbed. The active surface areas of various catalysts were calculated with this factor and are plott-

ed as a function of V_2O_5 loading in Figure 4. Other information derived from the LTOC data are given in Table 1.

DISCUSSION

Surface state and dispersion of V-oxide on γ-Al_2O_3.

The reducibility of the supported catalysts, as reflected by the extent of LTOC, shows a steady increase as a function of V_2O_5 content up to 11.9%, after which it decreases with loading. This behaviour is attributed to the formation of V-oxide monolayer due to carrier-catalyst interaction [2,3] in the lower loading region and the formation of crystallites by multilayer deposition of V-oxide on the monolayer at higher loadings. The decline in the reducibility of V-oxide in the 'post monolayer' region stems from the fact that in the bulky crystallites not all the V-oxide units are accessible to the reducing gas. On the other hand, in the monolayer region the maximum number of such units (not necessarily 100%) are available for reduction due to high dispersion.

ESR results offer strong evidence in favour of the above contention. In general, dipolar broadening leads to a singlet ESR spectrum when the paramagnetic species remain in close proximity with each other on a surface. Thus, Takahashi et al. [14] attribute the absence of hfs of crystalline V_2O_5 to the V^{4+} ions that remain as dense clusters. Conversely, the presence of hfs of supported catalysts can be taken as an indirect evidence for high dispersion that prevents the V^{4+} ions from coming close enough to give rise to dipolar broadening. This is the reason why γ-alumina supported V-oxides show hfs and the silica supported samples do not. The interaction between V-oxide and alumina is much higher than that between V-oxide and silica [14,15]. Our ESR results show that in the post monolayer region the hfs tend to diffuse, especially in the region with higher values of m_I, while within the monolayer region the spectra are well resolved (Figure 3). These observations led us to believe that V-oxide remains highly dispersed on alumina surface at the lower loading region.

The above arguments take on added weight from the results of surface area measurements. Massoth [17] showed with supported Mo oxide and sulfide catalysts that within monolayer limit the BET surface areas based on unit weight of support should remain constant and practically equal to that of the support; while that based on unit weight of the catalyst should decrease with increased load of the active component. Our results of similar calculations are depicted in Figure 1 where it is clearly seen that a monolayer is indeed formed at the lower loading region.

By defining dispersion as the percent of V-oxide units available for reduction and subsequent LTOC, it is possible to have an estimate of it from the total num-

ber of V-oxide units present in a sample and the number of oxygen atoms chemisorbed. With the assumption that one O atom corresponds to two V atoms as per the equations:

$$V_2O_5 + H_2 = V_2O_4\square + H_2O \quad (1)$$

$$V_2O_4\square + O = V_2O_5 \quad (2)$$

dispersion for all the supported catalysts have been calculated and are shown in Figure 4. From this figure it is observed, as expected, that dispersion remains constant in the monolayer region and decreases almost linearly as a function of V-oxide loading in the post monolayer region.

Active surface area and active site density

From the LTOC data the active surface areas of the catalysts were calculated and the results are shown in Figure 4. Again we see that active surface area increases in the monolayer region and decreases in the post monolayer region as a function of vanadia content. From the surface coverage data (Table 1) it is observed that even at the full monolayer coverage no more than about 22% of the support surface is occupied by the active component. A plausible explanation for such a low coverage could be that during the liquid phase preparation step the bulky polyvanadate ions failed to penetrate some micropores of the support [2,3]. Therefore, we depict the monolayer as isolated patches or islands of V-oxide units attached to the support surface by a strong chemical force. This chemical interaction is possible on a small fraction of the total surface of the support. The completion of the monolayer occurs when this active surface is covered completely by V-oxide. Any further addition of the active component leads to multilayer growth on the monolayer and eventual formation of bulky crystallites, while a large fraction of the carrier surface still remains bare. This observation agrees with the recent findings of Inomata et al. [18]. However, their data on the dispersion, crystallite formation etc., do not agree with ours. This difference might stem from the method of preparation, starting materials and characterization techniques which were different. These differences are reflected by the fact that their samples show XRD patterns starting from vanadia loading of about 48 weight % (corresponding to 35 mole %) as compared with 12% in our case.

With the above information on the surface state, dispersion and active surface areas of the catalysts, it is tempting now to elicit some information on the active site density on the surface. The active sites are envisaged as the vacancies created by the removal of labile oxygen atoms that take part in the redox [19] processes in oxidation reactions. By assuming dissociative chemisorption of oxygen on these vacancies (see Equations 1 and 2) the site densities have been calculated

from the BET surface areas of the reduced catalysts. The results are given in Table 1. As in the cases of active surface area and coverage, the active site density is found to increase in the monolayer level and decrease in the post monolayer level with increasing vanadia content.

ACKNOWLEDGEMENTS

We wish to thank Dr. G. Thyagarajan, Director of the RRL. Hyderabad, for permitting us to publish this work. Our thanks are also due to the University of Hyderabad and the GSI for allowing us to use the ESR and atomic absorption spectroscopy respectively. K.S. Rama Rao helped in conducting some experiments. KVRC and BMR are the recipients of CSIR fellowships.

REFERENCES

1 G.C. Bond, A.J. Sarkany and G.D. Parfitt, J. Catal., 57 (1979) 476.
2 F. Roozeboom, T. Fransen, P. Mars and P.J. Gellings, Z. Anorg. Allg. Chem., 449 (1979) 25.
3 F. Roozeboom, Ph.D. Thesis, Twente University of Technology (1980).
4 K. Tarama, S. Teranishi, S. Yoshida and N. Tamura, Proc. Intern. Congr., Catalysis, 3rd Amsterdam 1964, p.282, North Holland (1965).
5 K. Tarama, S. Yoshida, S. Ishida and H. Kakiota, Bull. Chem. Soc., Japan, 41 (1968) 2840.
6 B.S. Parekh and S.W. Weller, J. Catal., 47 (1977) 100.
7 H.C. Liu and S.W. Weller, J. Catal., 66 (1980) 65.
8 J.L. Garcia Fierro, S. Mendioroz, J.A. Pajares and S.W. Weller, J. Catal., 65 (1980) 263.
9 H.C. Liu, L. Yuan and S.W. Weller, J. Catal., 61 (1980) 282.
10 S.J. Tauster, T.A. Pecoraro and R.R. Chianelli, J. Catal., 63 (1980) 515.
11 A. Lopez Agudo, F.J. Gil Llambis, P. Reyes and J.L. Garcia Fierro, Appl. Catal., 1 (1981) 59.
12 W. Zmierczak, G. Muralidhar and F.E. Massoth, J. Catal., 77 (1982) 432.
13 E.P. Barrett, L.G. Joyner and P.H. Halenda, J. Amer. Chem. Soc., 73 (1951) 373.
14 H. Takahashi, M. Shiotani, H. Kobayashi and J. Shoma, J. Catal., 14 (1969) 134.
15 M. Akimoto, M. Ushami and E.Echigoya, Bull. Chem. Soc. Japan, 51 (1978) 2195.
16 S. Yoshida, T. Iguchi, S. Ishida and K. Tarama, Bull. Chem. Soc. Japan, 45 (1972) 376.
17 F.E. Massoth, J. Catal., 50 (1977) 190.
18 M. Inomata, K. Mori, A. Miyamoto and Y. Murakami, J. Phys. Chem., 87 (1983) 761.
19 P. Mars and D.W. Van Krevelen, Chem. Eng. Sci., 3 (1954) 41; Spc. Suppl. Proc. Conf. Oxid. Processes 1954.